

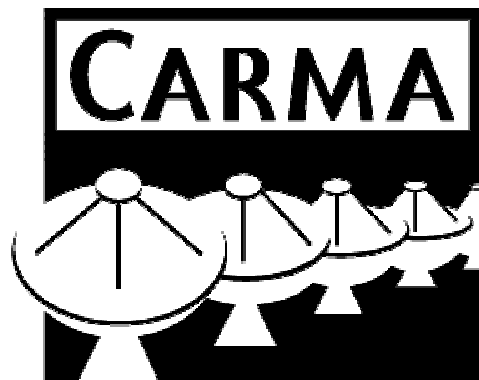
**CARMA Memorandum Series #32**

**Preliminary test results of the turnstile junction  
waveguide orthomode transducer for the 1 mm band**

A. Navarrini, A. Bolatto and R. L. Plambeck

*Radio Astronomy Lab, University of California, Berkeley*

March 15<sup>th</sup>, 2006



Combined Array for Research  
in Millimeter-Wave Astronomy

---

# Preliminary test results of the turnstile junction waveguide orthomode transducer for the 1 mm band

## Abstract

*We tested five prototype waveguide orthomode transducers (OMTs) designed for the 200-270 GHz frequency band. These OMTs, based on a turnstile junction, have identical designs (Navarrini et al. 2005), but were fabricated by different manufacturers using different techniques and materials. The OMTs were tested at NRAO, Charlottesville, using a Vector Network Analyzer (VNA) in the frequency range 210-310 GHz. Three of the OMTs have average room temperature insertion loss of ~1 dB or better, average input and output reflection of approx -18 dB, and cross-polarization and isolation of order -30 dB over 210-270 GHz.*

*The integrity of the tuning stub in the turnstile junction is the key for good performance: a gap between the quadrants there causes additional losses up to several tenths of a dB. Filling up the gap with indium gave, for the OMT with best performance, a transmission loss better than -0.8 dB over the entire 210-290 GHz band. Input and output reflections are better than -12 dB, with cross-polarization and isolation better than -25 dB across the same band.*

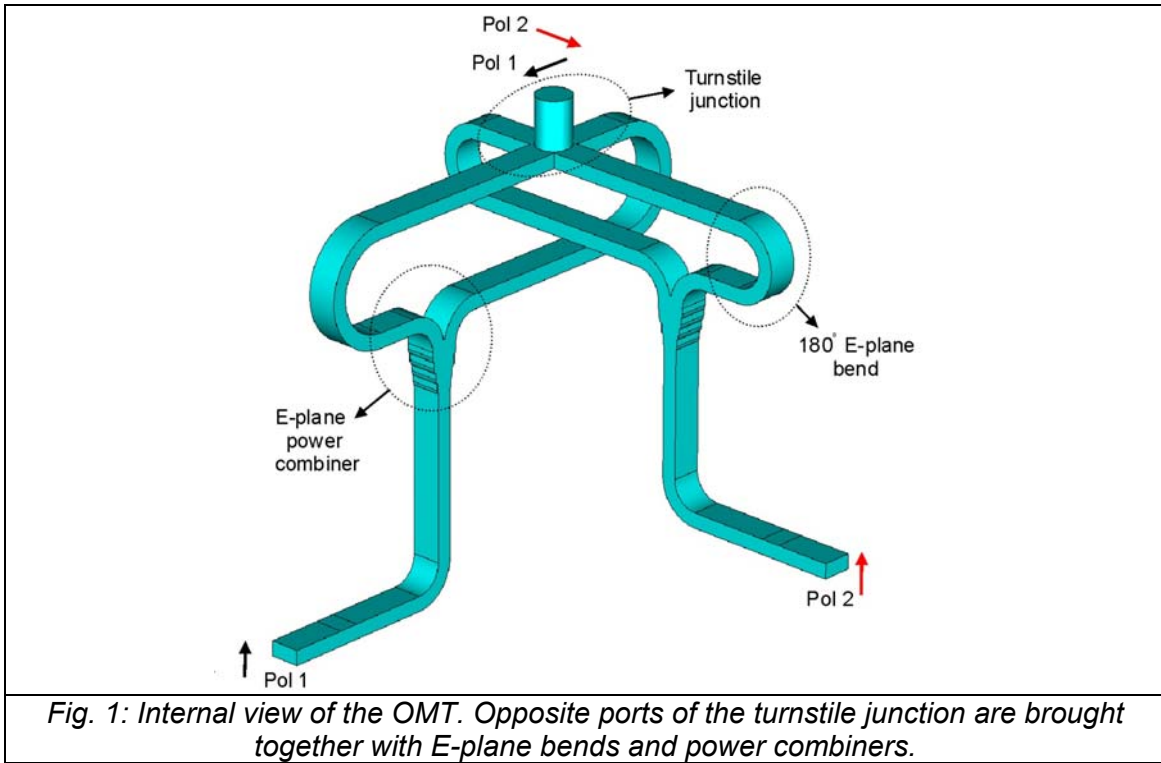
*Two of the OMTs had problems, showing narrow and deep transmission resonances in the band of interest. Modeling at 1 mm and experimentation with a K-band scale model of the OMT indicate that these resonances are probably related to fabrication errors that cause a misalignment of one (or more) of the four quarters of the OMT. These misalignments change the electrical path length of the waveguide between the turnstile junction and one of the power combiner inputs, causing a phase difference between the sidearms of the turnstile junction that gives rise to reflections in the power combiner.*

## 1 Introduction

We are constructing OMTs for dual polarization 200-270 GHz receivers on the CARMA array. The design of the OMT is discussed in [1] and [2]. The device has a circular waveguide input (diameter 0.044") and two WR3.7 rectangular waveguide outputs (0.0370"× 0.0185"). The OMT, illustrated in Fig. 1, utilizes a turnstile junction and two E-plane power combiners [3]. A tuning stub located at the base of the circular waveguide matches the input over a full frequency band.

## 2. Mechanical blocks

The OMT is constructed by dividing the structure of Fig. 1 into four blocks that intersect along the circular waveguide axis. The tuning stub at the base of the turnstile junction is split into four identical sections that are machined at the same time as the rectangular waveguides. The OMT, shown in Fig. 2, accepts a standard UG387 flange at its input so it can mate with our existing feed-horns.



Custom mini-flanges are used for the WR3.7 output waveguides of the OMT for compactness of the device. The mini-flanges are identical to those of the ALMA Band 6 OMTs and SIS mixers, where the alignment pins and screw holes are on a 0.280" diameter bolt circle. Our OMT is a cube 0.9" on a side. The electrical

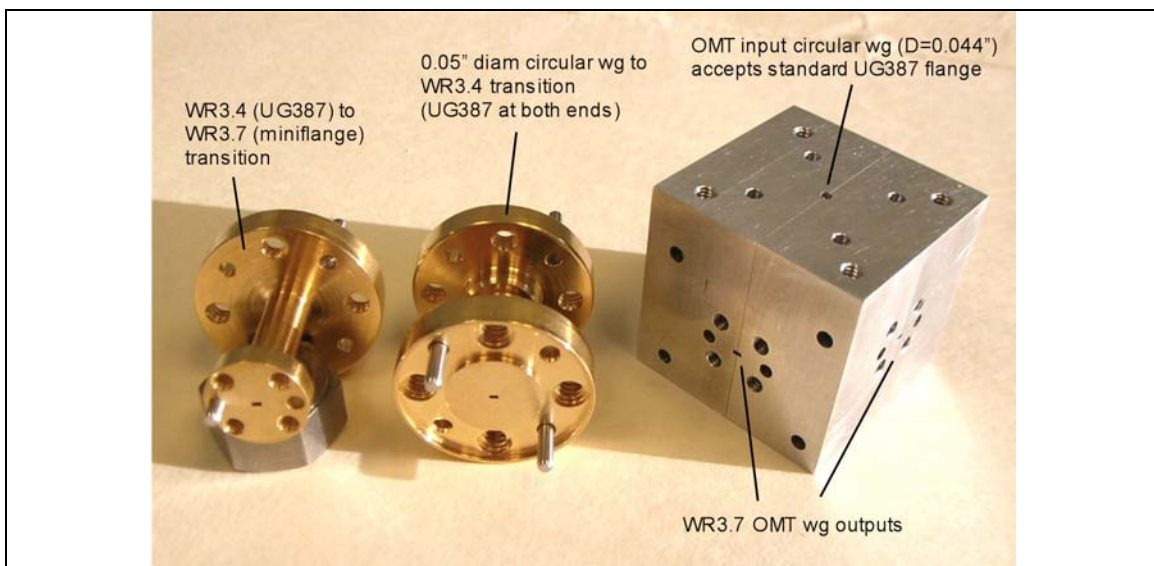


Fig. 2. View of assembled OMT (on the right) with its circular waveguide input on top and the two WR3.7 waveguide outputs with custom mini-flanges. Two of the 0.75" long transitions used to test the OMT are shown on the left of the OMT.

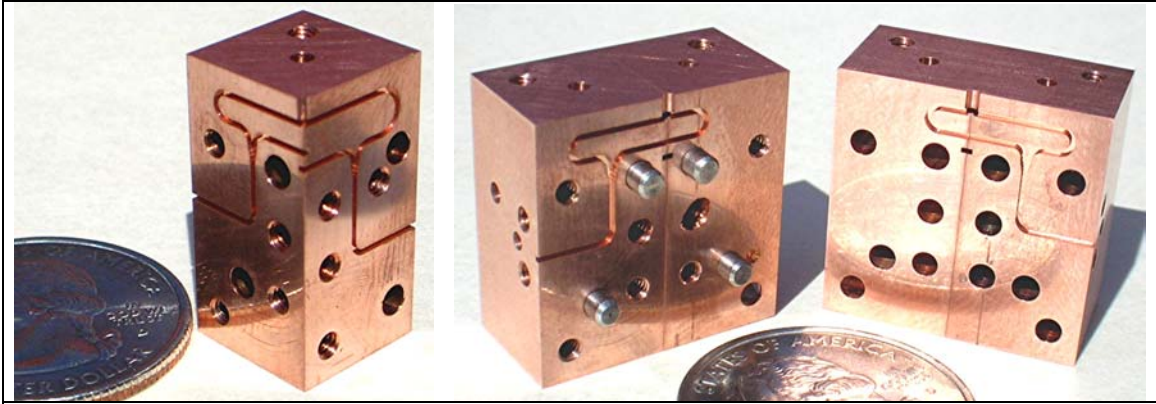


Fig. 3. OMT n. 2 machined at RAL. *Left)* View of one of the four blocks. *Right)* View of assembled mating pairs of blocks showing the waveguide circuitry for Pol 2.

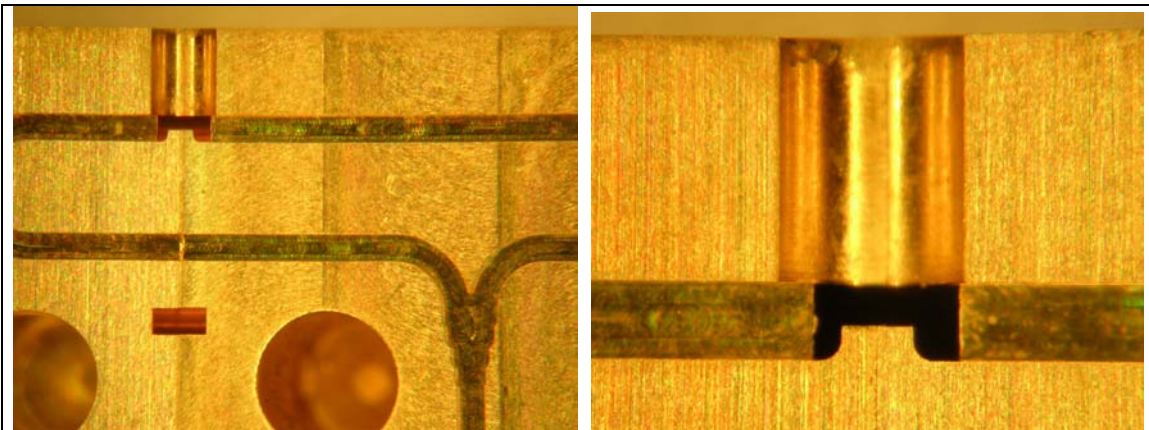


Fig. 4. OMT n. 5 machined at Univ. of Arizona. View of an assembled mating pair of blocks showing the internal waveguide circuitry of turnstile junction, and power combiner (on the left), and the details of the tuning stub at the turnstile junction circular waveguide base (on the right).

**Table 1:**

OMT n.	Machined by	Material	Notes
1	RAL, Berkeley, CA	Aluminum	Four blocks machined from a single bar
2	RAL, Berkeley, CA	TeCu	Four blocks machined from a single bar
3	Protofab, Petaluma, CA	TeCu	Blocks machined individually
4	Custom Microwave Inc., Longmont, CO	Gold plated brass	Blocks machined individually. Plating type: STM B4488. Gold thickness=20-30 $\mu\text{in}$ , 99.7% pure gold (no Nickel)
5	University of Arizona, Tucson, AZ	Gold plated brass	Blocks machined individually. Plating MIL-G-4S204C Type III, Grade A, Class 0, 99.99% pure gold. 20 $\mu\text{in}$ of Nickel+30 $\mu\text{in}$ of gold. Tuning stub damaged during plating. Loose alignment pins

path length from the circular waveguide at the input of the OMT to the WR3.7 waveguide outputs is ~1.1" for Pol 1 and ~1.2" for Pol 2.

Fig. 3 shows photos of one of the four blocks and of the mated block pairs. Details of the internal waveguide circuitry of the OMT are shown in the photos of Fig. 4.

Five OMTs of identical design were fabricated by different manufacturers using different materials and machining techniques. Their main features are summarized in Table 1. Measurement results allowed to compare OMTs performance in relation to mechanical tolerances.

The four blocks of OMTs n. 1 and n. 2 were machined in our own shop at one time as part of a single 0.5"x0.5"x6.5" metal bar using a numerically controlled milling machine (CNC Tree Journeyman 350 equipped with high speed Astro-E500 spindle 50000 rpm.) Inspection of the blocks with the optical microscope showed that the maximum offset between rectangular waveguide cuts in block halves is approximately 0.0015". The four blocks of the other three OMTs were fabricated individually using machines capable of achieving better accuracy. The maximum offset between waveguide cuts in block halves of OMT n. 5, fabricated at University of Arizona using a Kern Micro milling machine, was less than 0.0006". Unfortunately, the tuning stub and one of the power combiners of such OMT were slightly damaged after we sent it out for gold plating.

### 3 Measurement setup

We tested the five OMTs during the week 24-28 October 2005, at NRAO,

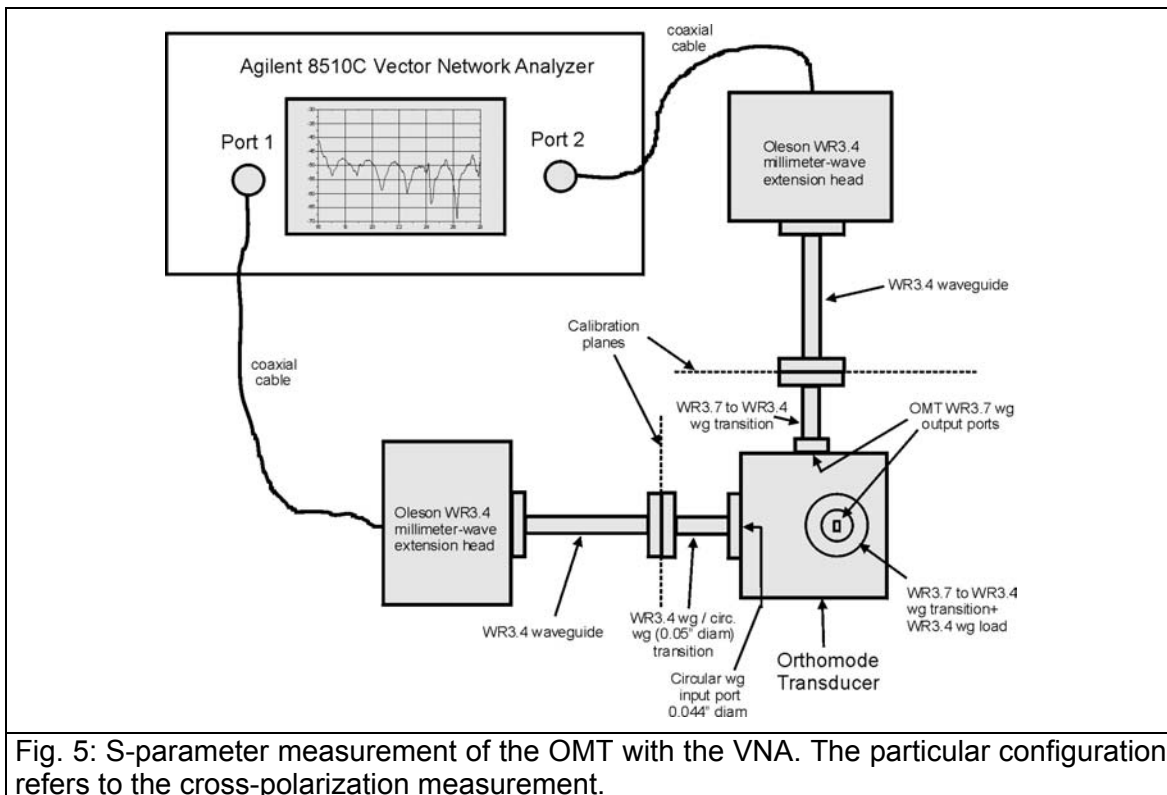


Fig. 5: S-parameter measurement of the OMT with the VNA. The particular configuration refers to the cross-polarization measurement.

Charlottesville, using an Agilent 85106C Vector Network Analyzer (VNA) equipped with Oleson WR3.4 millimeter-wave test set extensions. A schematic of the cross-polarization test setup is shown in Fig. 5. The VNA was calibrated at the WR3.4 waveguide at the outputs of the extension heads using a two-port TRL calibration with Oleson WR3.4 calibration kit. A Custom Microwave transition from WR3.4 rectangular waveguide to 0.050" diameter circular waveguide (Fig. 2) was attached to the 0.044" circular waveguide input of the OMT. Although the locating pins of the OMT input flange are on the normal 0.562" diameter bolt circle, it was not possible to locate the waveguide screws in their normal positions, so a special aluminum clamp was made to bolt the OMT to the flange of the transition (Fig. 6.) One of the two OMT WR3.7 rectangular waveguide outputs was connected to the WR3.4 waveguide section attached to the mm extension head through a Custom Microwave WR3.7 to WR3.4 waveguide transition (with custom mini-flange on the WR3.7 side and standard UG387 flange on the WR3.4 side.) The second OMT output was terminated with a WR3.4 waveguide load through an identical WR3.7 to WR3.4 waveguide transition. Pol 1 or Pol 2 was excited by rotating the input transition by 90° at the circular flange.

The calibration procedure was used to remove systematic instrumental effects and to calibrate out the response of the instrument up to the WR3.4 waveguides attached to the millimeter-wave extension heads. Additional measures of two pairs of identical transitions back to back allowed to calibrate

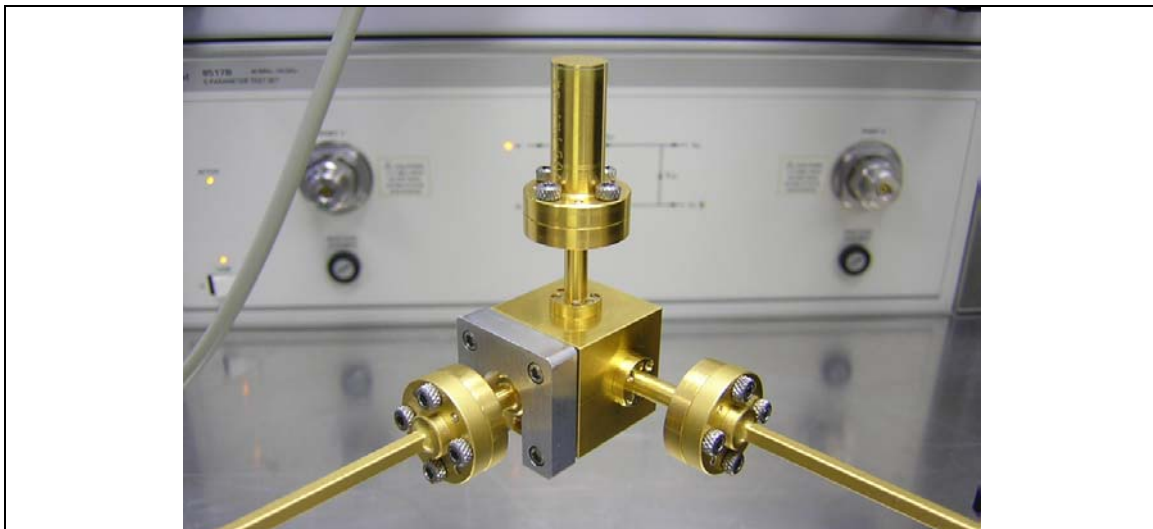


Fig. 6. Pol 1 transmission measurement of the OMT with the VNA. An aluminum clamp is used to attach the WR3.4 to 0.050" diameter circular waveguide transition at the input of the OMT (on the left.) One of the OMT WR3.7 output is attached to the WR3.4 waveguide connected to the mm-wave extension head of the VNA through a WR3.7 to WR3.4 transition (on the right.) The second OMT WR3.7 output (on top) is terminated into a WR3.4 waveguide load through a WR3.7 to WR3.4 transition. A single two-port measurement in this configuration provides the direct and reverse transmission as well as the input and output reflection of the OMT with transitions.

out their individual effects and to derive the S-parameters of the OMTs at the physical ports of the device. The TRL calibration uses a 0.1001” shim for the THRU, 0.1001” +  $\lambda/4$  (0.1147”) shim for the LINE/REFLECT, and no shim for the port 1 and port 2 SHORT. The IF averaging factor was set to 256. We checked the calibration regularly during the day after having completed the full set of S-parameters measurement of each OMT. The calibration was stable for four days. Some of the measurements required to flip by 90° the millimeter heads of the VNA; we checked that neither flipping nor moving the heads affected the calibration. We repeated the measurement of one same OMT at different times and confirmed that the measurement repeatability error was a minor contribution to the total error in the measurement.

## 4 Experimental results

We tested the OMTs between the minimum operating frequency of the VNA, 210 GHz, up to 310 GHz. This range overlaps with most of our OMT design band, 200-270 GHz. Between 210-215 GHz the measurements have a higher noise level because of the lower power level of the VNA in that frequency range.

Tests of the OMTs showed that their good performance depends on the integrity of the tuning stub located at the base of the circular waveguide. Three of the OMTs had small imperfections and gaps between quadrants at the tuning stub. After filling the gap with indium, the insertion loss improved by several tenths of a dB. Here, we present the results for the transmission loss before and after tuning stub fix.

### 4.1 Transmission measurements of OMTs before tuning stub fix

The transmission measurements of the five OMTs before tuning stub fix are given in Figs. 7-8. The vertical line in the graphs delimits the nominal highest frequency of the band at 270 GHz. OMTs n. 3 and 4 gave the best performances with transmission levels above -1.3 dB across 210-270 GHz. Only Pol 1 transmission was measured for OMTs n. 1 and 5. The insertion loss of OMT n. 1 is in the range 1-2 dB across 210-270 GHz. Over most of the same frequency band, polarization channel 2 of OMT n. 2 has a flat transmission with value -1.5 dB. The other polarization channel, Pol 1, shows resonances across the band with depth down below the -4 dB level. Also, Pol 1 of OMT n. 5 shows deep resonances across the band. Electromagnetic simulations show that the resonances are due to a difference in electrical length between turnstile junction sidearms. We will discuss the origin of the resonances in the next section.

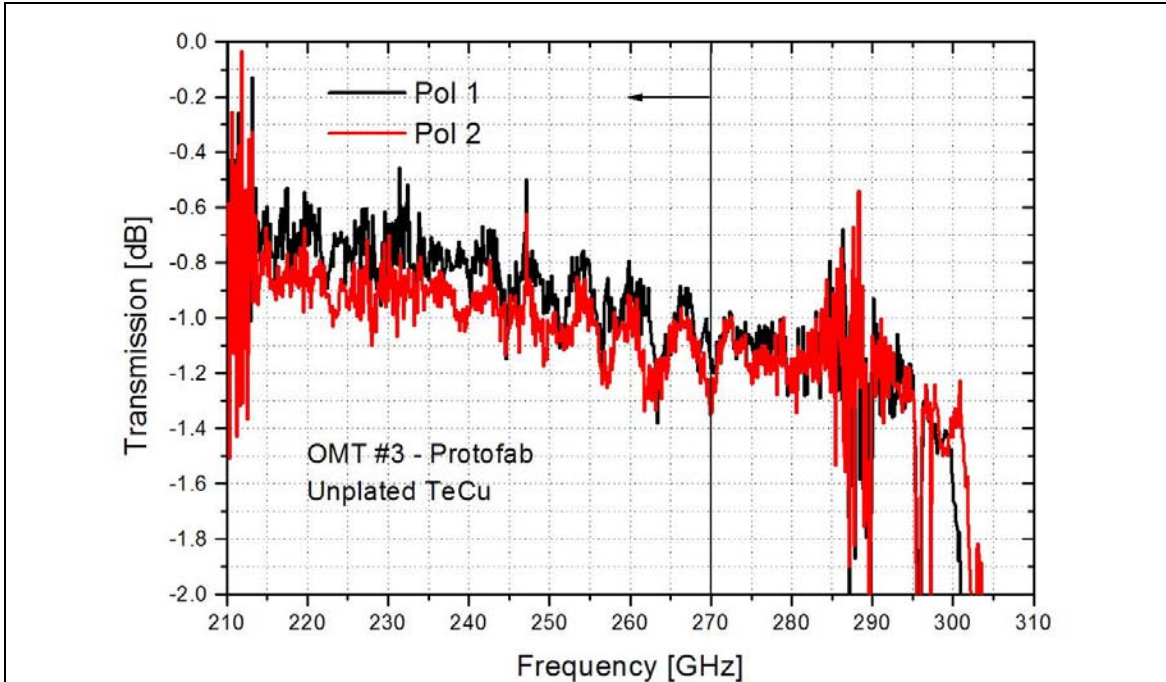


Fig. 7: Pol 1 and Pol 2 transmission measurement of OMT n. 3 before tuning stub fix.

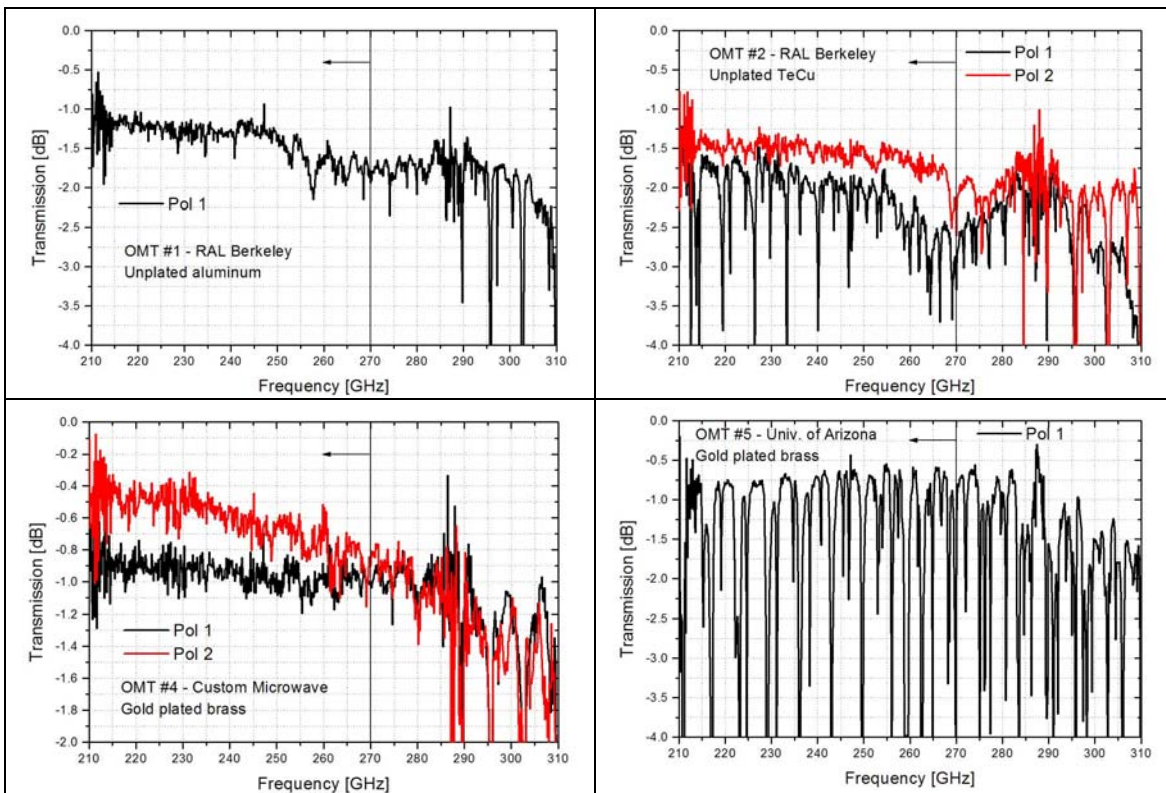


Fig. 8: Transmission measurement before tuning stub fix of OMT n. 1 (top left), n. 2 (top right), n. 4 (bottom left), n. 5 (bottom right). Note that the tuning stub and power combiner of OMT n. 5 were slightly damaged during gold plating. Also, loose locating pins were used, which may have caused a lateral misalignment between block halves and originated the deep resonances observed in the transmission.

#### 4.2 Transmission measurements of OMTs after tuning stub fix

The measurements were repeated after tuning stub fix by filling small imperfections and gaps between quadrants with indium. Fig. 9 shows photos of the tuning stub of OMT n. 3 before and after the fix. After fix, the insertion loss of

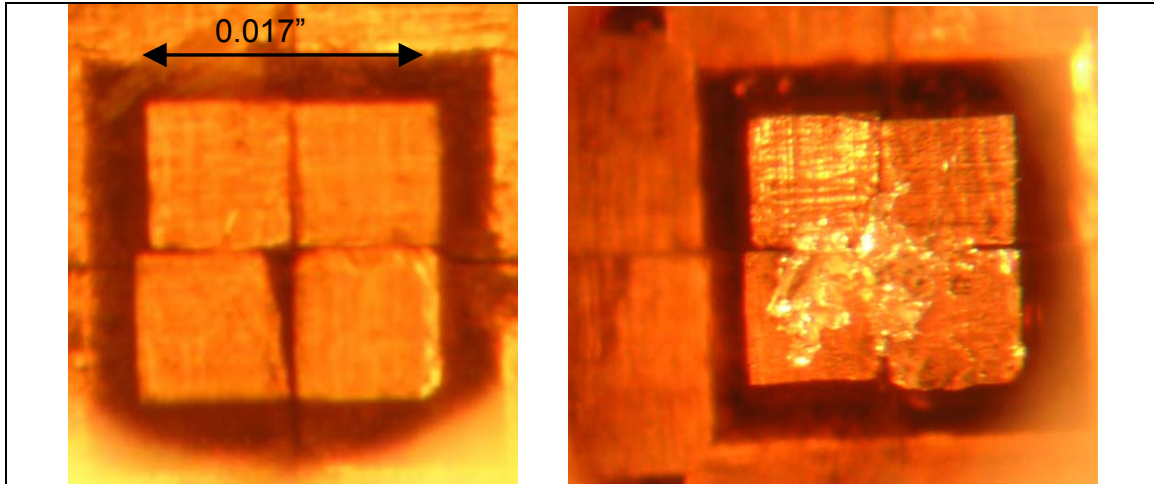


Fig. 9. Magnified top view of the tuning stub before (left) and after (right) filling up the gap with indium of OMT n. 3. After tuning stub fix, the value of insertion loss of this OMT improved by approximately 0.4 dB across the band.

the OMTs improved by several tenths of a dB in most cases. Figs. 10-11 show the transmission of the five OMTs. Both polarization channels of OMT n. 3 improved from an average value across the band of  $\sim 1$  dB (before tuning stub fix) to a value of  $\sim 0.6$  dB (after tuning stub fix), similar in overall level to the value predicted by the electromagnetic simulation. The measured transmission, shown in Fig. 10, is above  $-0.8$  dB across 210-290 GHz.

Ideally, the fix would require only a minimum amount of indium to exactly fill the gaps and the small imperfections at the tuning stub. OMT n. 4 showed no improvement of its performance after the fix because an extra amount of indium was used that slightly altered the dimensions of the stub from its ideal shape.

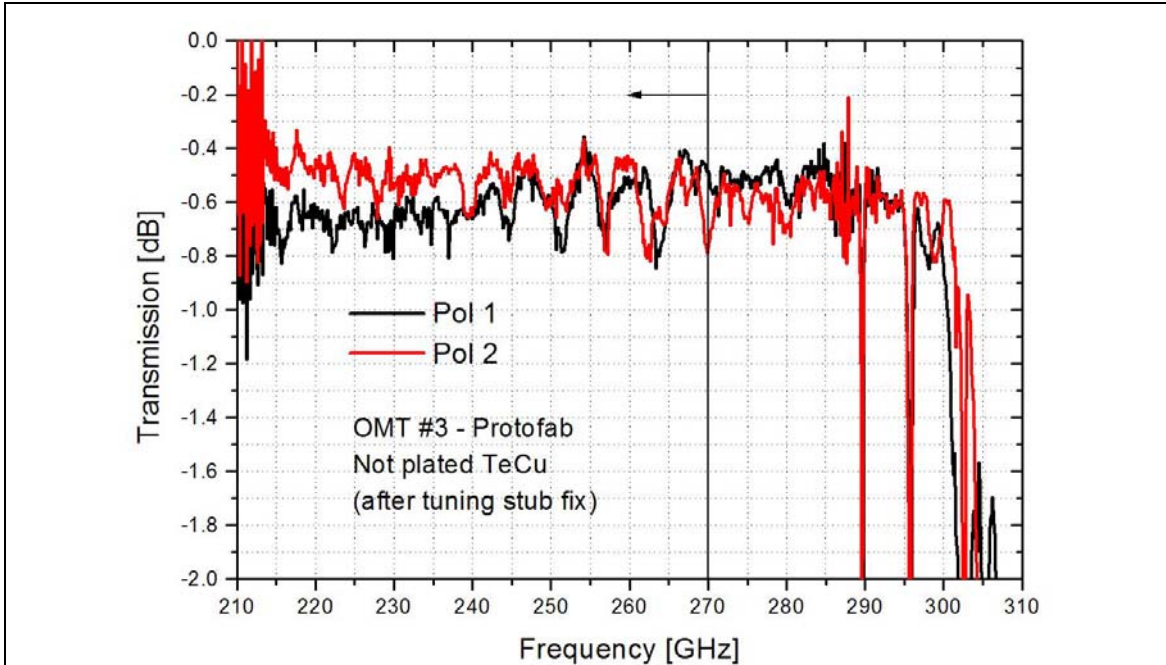


Fig. 10: Pol 1 and Pol 2 transmission measurement of OMT n. 3 after tuning stub fix.

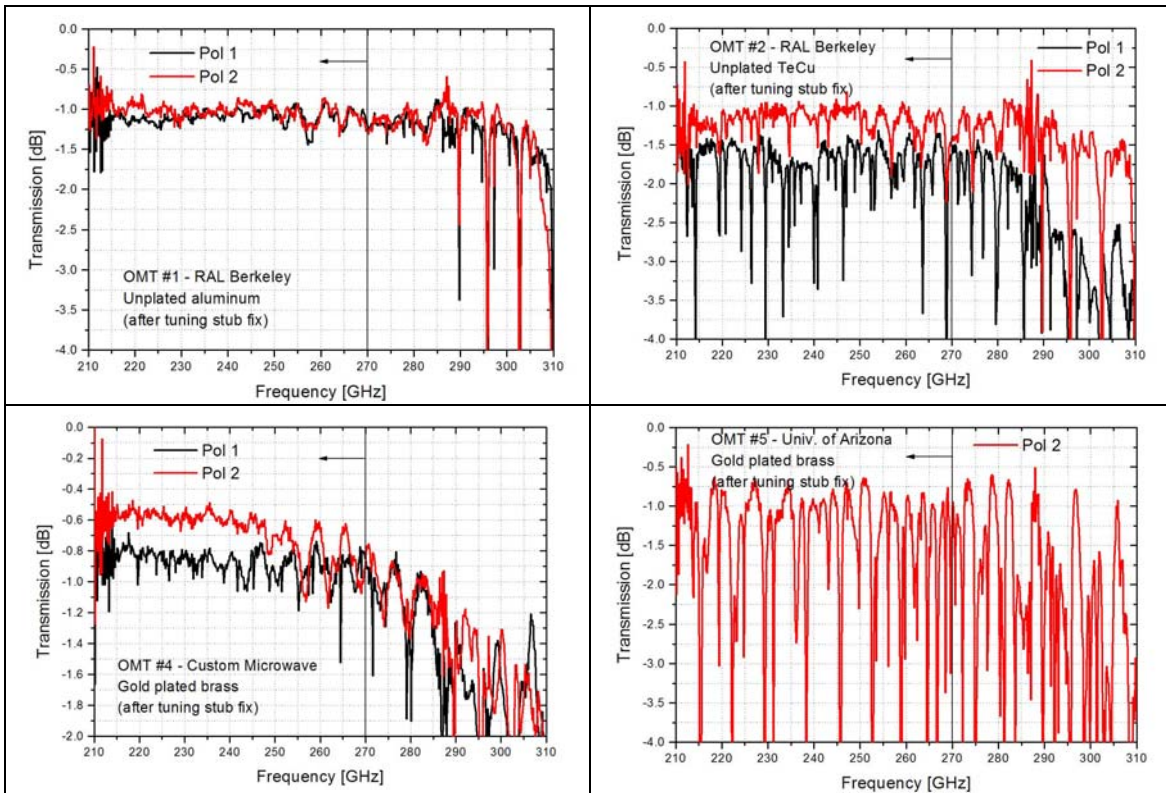


Fig. 11. Fig. 8: Transmission measurement after tuning stub fix of OMT n. 1 (top left), n. 2 (top right), n. 4 (bottom left), n. 5 (bottom right). Deep resonances are seen in both polarizations channels of OMT n. 5.

### 4.3 Reflection, cross-polarization and isolation measurements of OMTs

Figs. 12-14 show, respectively, the measured input reflection, the cross-polarization, and the isolation of OMT n. 4 before tuning stub fix. The reflection at the input ports is below  $-14$  dB across 210-290 GHz and closely resembles that measured at the output ports (not shown.) The cross-polarization coupling and the isolation between output ports are below  $-27$  dB across the same band.

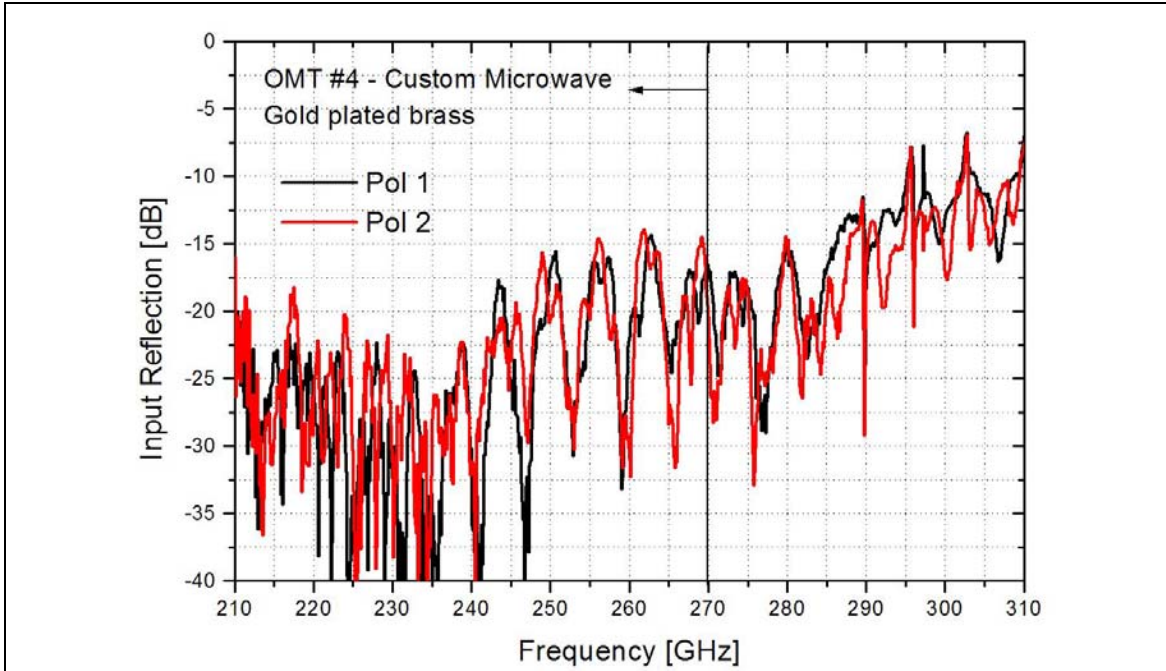


Fig. 12. Pol 1 and Pol 2 input reflection measurement of OMT n. 4.

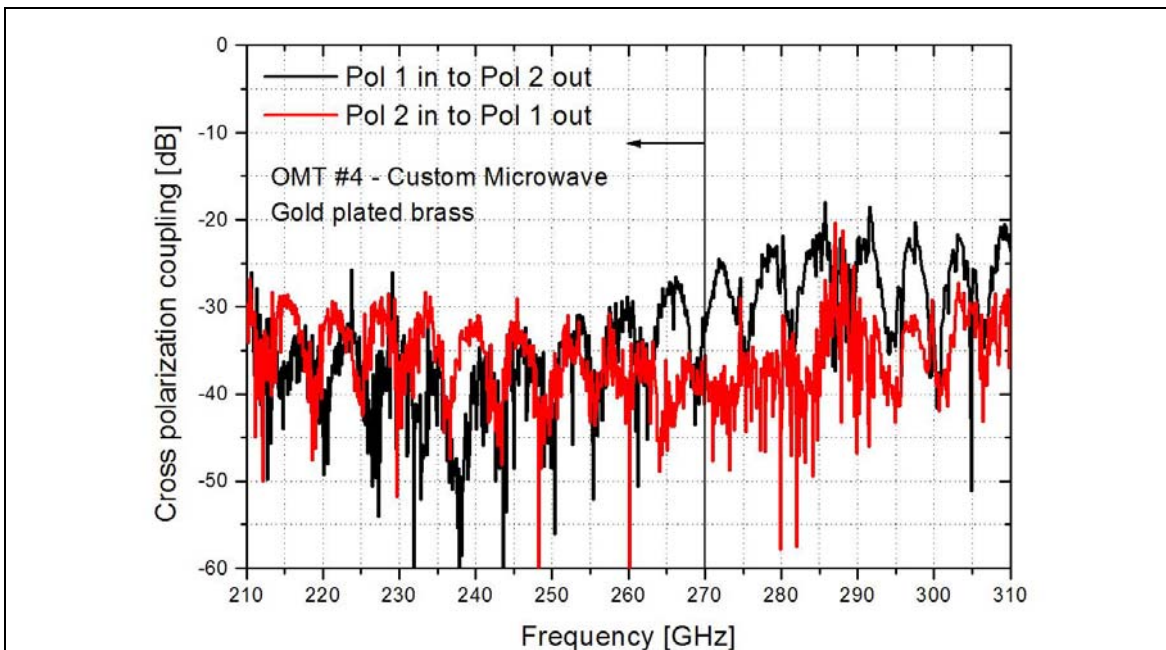


Fig. 13. Pol 1 and Pol 2 cross polarization measurement of OMT n. 4.

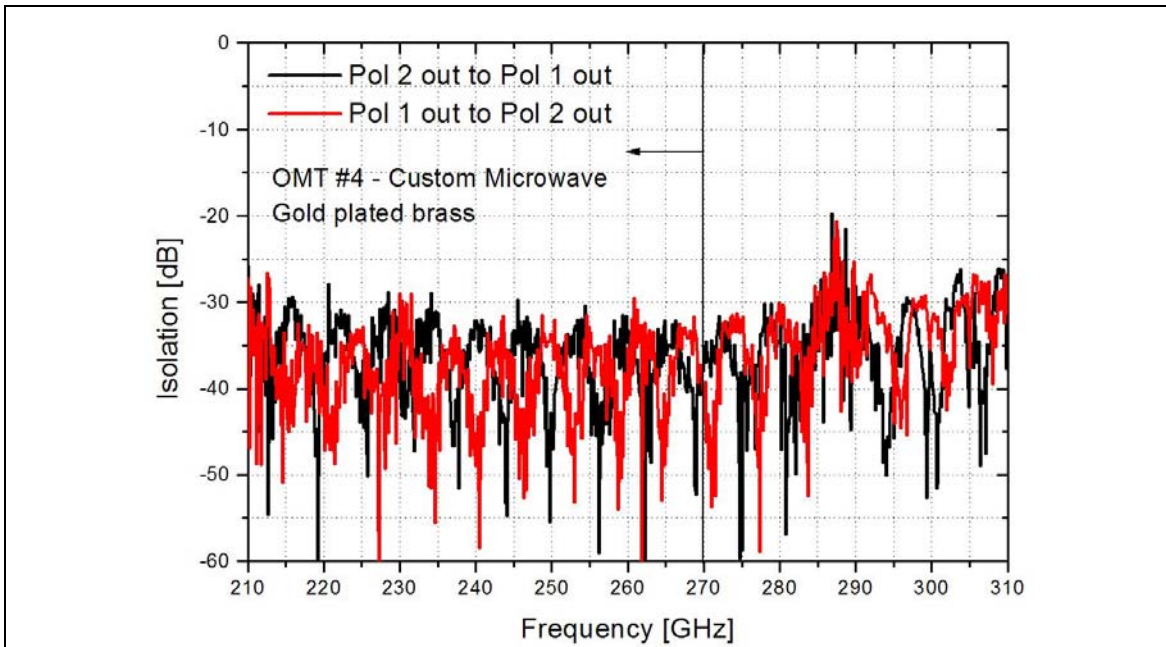


Fig. 14. Measured isolation between output ports for OMT n. 4.

Figs. 15-18 show the measured reflection, cross-polarization, and isolation for both polarization channels of OMT n. 3 after tuning stub fix. The input and output reflections are below  $-12$  dB across 210-290 GHz, unchanged before and after fix. The small differences between the measured reflection coefficients for the two polarization channels indicate that they are electrically very similar. The cross-polarization and isolation are both below  $-25$  dB; one of the two polarization channels improved by  $\sim 5$  dB after fix, bringing the average levels across the band from  $-30$  dB down to  $-35$  dB (Fig. 17 and Fig.18).

The input and output reflection of OMTs n. 1 and n. 2 are both below  $-10$  dB across 210-290 GHz. The cross-polarization and isolation are below  $-20$  dB over most part of the same band.

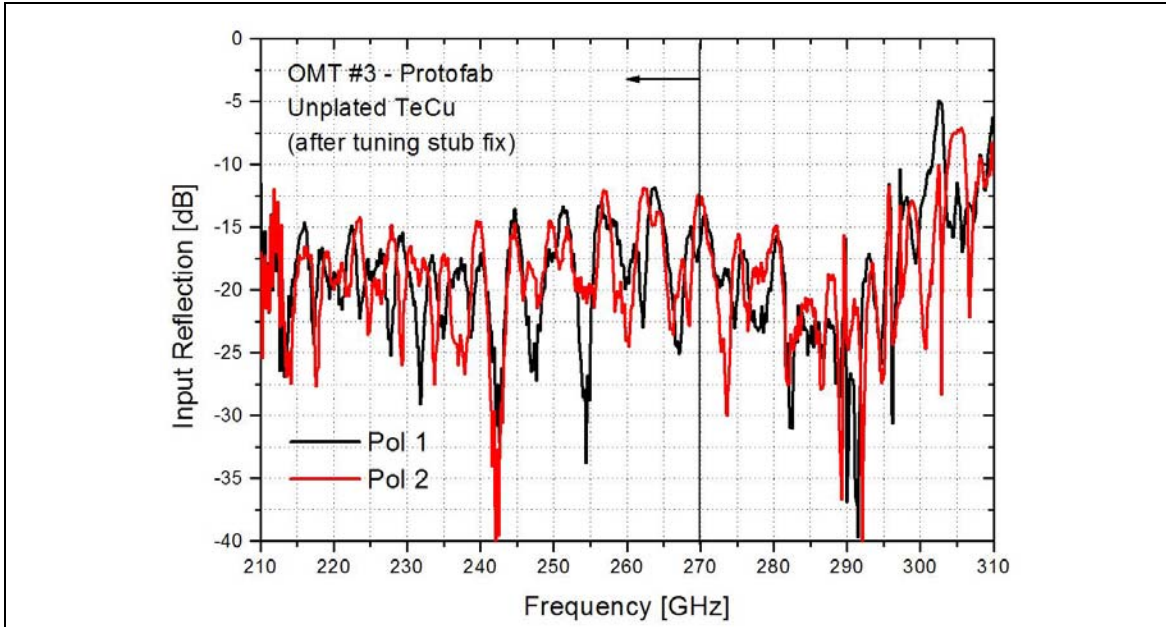


Fig. 15. Pol 1 and Pol 2 input reflection measurement of OMT n. 3 after tuning stub fix.

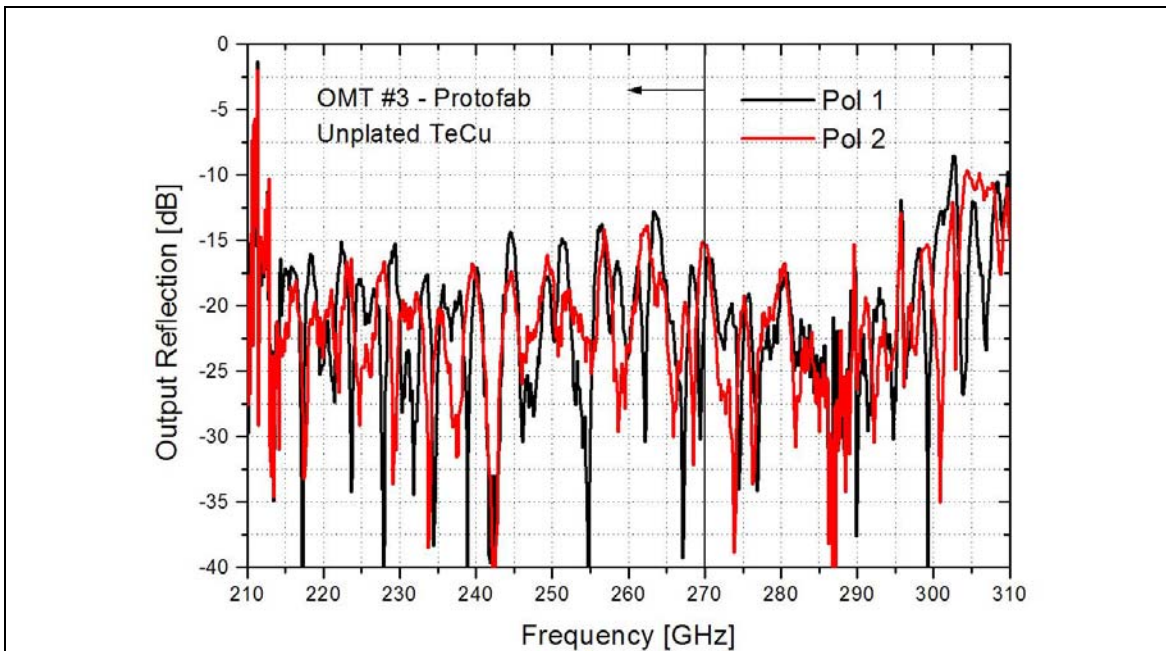


Fig. 16. Pol 1 and Pol 2 output reflection measurement of OMT n. 3 after tuning stub fix.

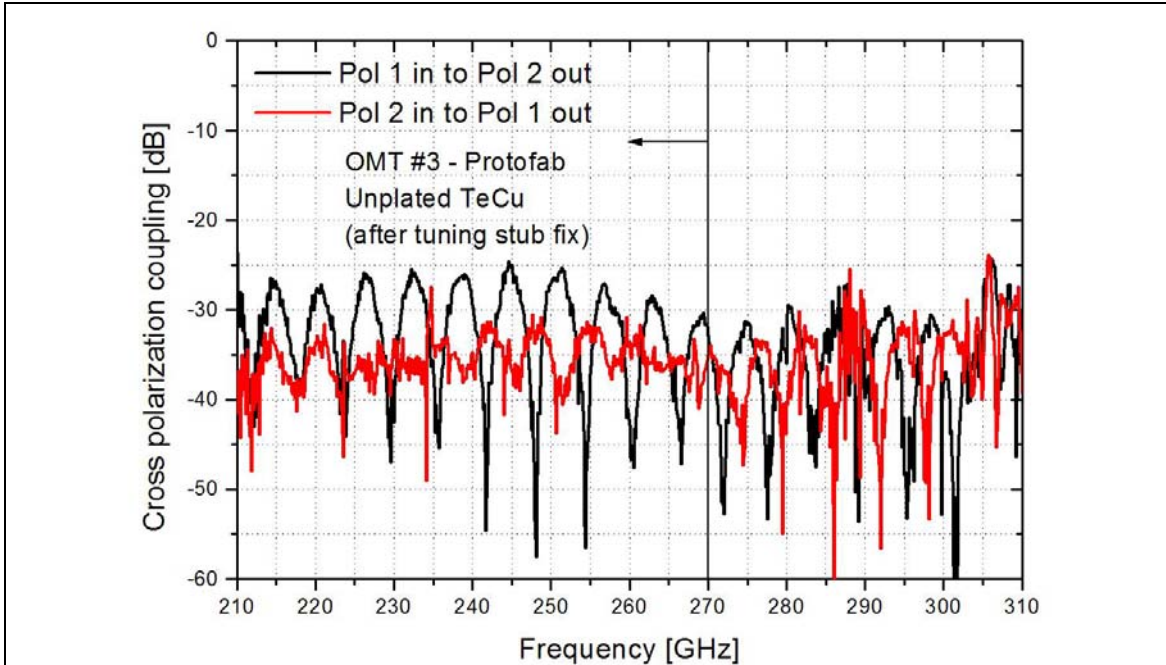


Fig. 17. Pol 1 and Pol 2 cross polarization measurement of OMT n. 3 after tuning stub fix.

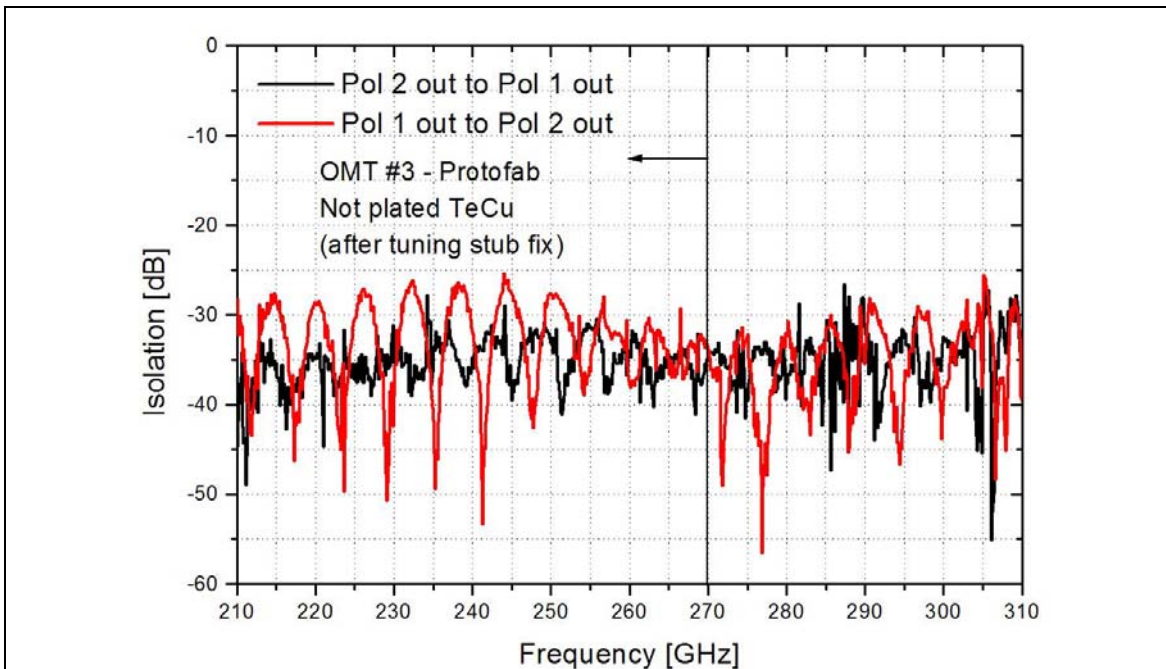


Fig. 18. Measured isolation between output ports for OMT n. 3 after tuning stub fix.

## 5 Dependence of performance on mechanical tolerances

The alignment of the four blocks and the integrity of the tuning stub are critical to the performance of the OMT. Misalignment of the blocks due to fabrication tolerances are thought to be the cause of the deep resonances measured in the transmission of OMTs n. 2 and n. 5. To estimate the degradation in performance due to fabrication tolerances we did numerical simulations of the full OMT structure with 0.001" errors.

A difference in the physical length of opposite waveguide arms between the turnstile junction and the power combiner causes the appearance of a series of resonances in the transmission of the OMT. Energy coming from the turnstile junction reflects back from the power combiner when the two signals reaching it are not exactly  $180^\circ$  out of phase. Electromagnetic simulations of the three-port model of Fig. 1 were performed with CST Microwave Studio [4] for balanced (ideal case) and imbalanced waveguide sidearm lengths with 0.001" length difference. We assumed the blocks to be gold plated with pure gold and used a gold conductivity of half its dc value ( $\sigma_{Au}=4.26 \cdot 10^7$ )/2  $\Omega^{-1}m^{-1}$ . For the ideal OMT, the simulated insertion loss, shown in Fig. 19, is  $\sim 0.65$  dB across the band, similar to the measured value. For the OMT with imbalanced sidearms, the simulation shows deep resonances across the band. The depth of the resonances increases with sidearm length difference; an increase of the waveguide losses makes the resonances shallower and broader.

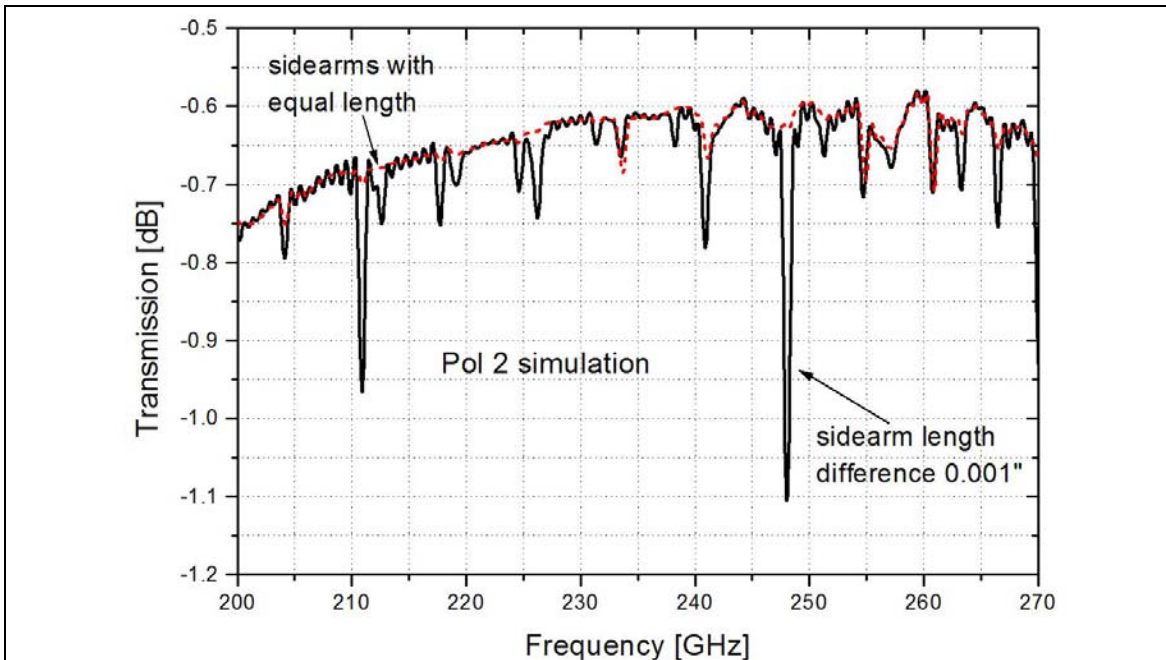
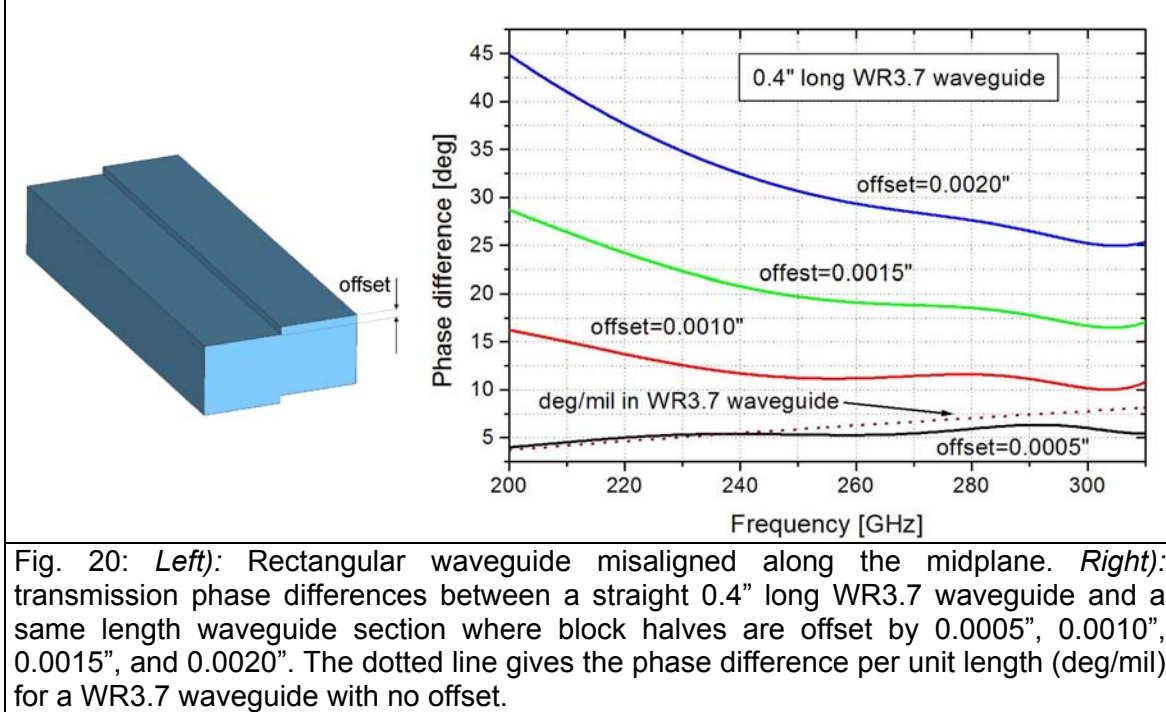


Fig. 19: Simulated room temperature transmission losses for Pol 2 of the OMT. The dashed line refers to the ideal three-port device illustrated in Fig. 1, with identical sidearms length. The solid line refers to a model where the length of one of the turnstile junction sidearms associated with Pol 2 is increased by 0.001".

Resonances in the transmission of the OMT are also expected when the physical length of the two waveguide sidearms is identical, but one of the sidearms has a different electrical length from the other: an offset along the midplane of the rectangular waveguides caused by a lateral misalignment of block halves, changes the propagation constant (and hence the phase velocity) with respect to a waveguide with no offset. Thus, if one of the four blocks of the OMT is offset along the circular waveguide axis, the two waveguide sidearms of each polarization channel will have different electrical lengths. Because of the different physical length of WR3.7 waveguide sections in different blocks, the electrical length difference depends on which one of the four blocks is offset with respect to the others. For example, an offset of the block having the shortest waveguide cut sections (the one without power combiners), causes an offset along the midplane of a ~0.4" long section of WR3.7 waveguide associated to polarization channel n. 1 on one of the lateral sidearms, but not on the other (the physical length of the sidearms between the turnstile junction and the power combiner is ~0.55" and ~0.50" for, respectively, polarization channels 1 and 2 of the OMT.) To give an estimate of the electrical length difference between two sidearms caused by an offset of one of the blocks along the axis of our OMT, we performed electromagnetic simulations of: *a)* a straight 0.4" long section of WR3.7 waveguide; *b)* a same waveguide length laterally misaligned along the midplane by 0.0005", 0.0010", 0.0015", and 0.0020" (see Fig. 20.) The difference between the phase of the two transmissions is ~12 deg at 230GHz for an offset of 0.0010". Notice that at the same frequency, the phase difference between two WR3.7 waveguides with length difference 0.0010" is ~5 deg/mil, less than half that value (Fig. 20, dotted line.) Therefore, a given amount of misalignment of one of the blocks along the circular waveguide axis (caused, for example, by loose locating pins) is expected to be more harmful to the OMT performance than fabrication errors causing a same amount of length difference between turnstile junction waveguide sidearms (Fig. 19, imbalanced case).

Electromagnetic simulations of the OMT with one misaligned block, as well as experimentation with the K-band OMT prototype, confirm that misalignments such as those described above are the cause of the deep resonances observed in some of the 1mm-band prototypes. Use of dowel pins and holes with a tight fit in the inner part of the OMT may help to reduce the misalignments between mating pairs of blocks. The graph on Fig. 20 shows that the phase difference increases with the offset. Simulations of the full OMT structure confirm that the depth of the resonances in the transmission increase when increasing the amount of offset.



## 5 Impact of OMT performance

A feed-horn with circular waveguide output (0.050" diameter) will attach to the circular waveguide input of the OMT (0.044" diameter.) Two Double Side Band (DSB) SIS mixers will be attached to the OMT WR3.7 waveguide outputs. Insertion losses in the OMT increase the noise temperature  $T_{\text{rec}}$  (referred at the receiver input) of the dual-polarization DSB receiver. The losses associated with infrared filtering, local oscillator injection, telescope spillover and atmospheric attenuation also contribute to degrade the actual figure of merit for astronomical spectroscopy: the SSB system noise temperature of the DSB receiver. Referring the system noise outside the atmosphere, this can be expressed in a simplified form as:

$$T_{\text{sys,SSB}}^* = (2/\eta_F) [T_{\text{rec}} e^{A\tau} + (1-\eta_F) T_{\text{amb}} e^{A\tau} + \eta_F (e^{A\tau} - 1) T_{\text{atm}}]$$

where  $\eta_F$  is the forward efficiency,  $\tau$  is the atmospheric transmission,  $T_{\text{amb}}$  is the termination of spillover losses,  $T_{\text{atm}}$  is the termination of atmospheric losses, and  $A$  is the airmass of the source. We use the above equation to estimate the noise temperatures  $T_{\text{rec}}$  and  $T_{\text{sys,SSB}}^*$  as a function of the insertion loss at 4 K due to the OMT. Fig. 21 shows the increase of receiver noise and system noise versus insertion loss. The increase of receiver and system noise temperature relative to an ideal case where a lossless OMT is used, is given on Fig. 22. For these calculations we have assumed the following values:  $T_{\text{rec}}(\text{IL}=0 \text{ dB})=30 \text{ K}$  (receiver with ideal, lossless, OMT),  $T_{\text{amb}} = 280 \text{ K}$ ,  $T_{\text{atm}} = 250 \text{ K}$ ,  $\eta_F = 0.95$ ,  $\tau=0.2$ , and  $A=1.414$  (observation at  $45^\circ$  elevation). The resulting  $T_{\text{sys,SSB}}^*(\text{IL}=0 \text{ dB})= 286 \text{ K}$ . The insertion loss of the OMT is expected to decrease by a factor of  $\sim 3$  when it is cooled to cryogenic temperatures [5]. Therefore, assuming the room temperature

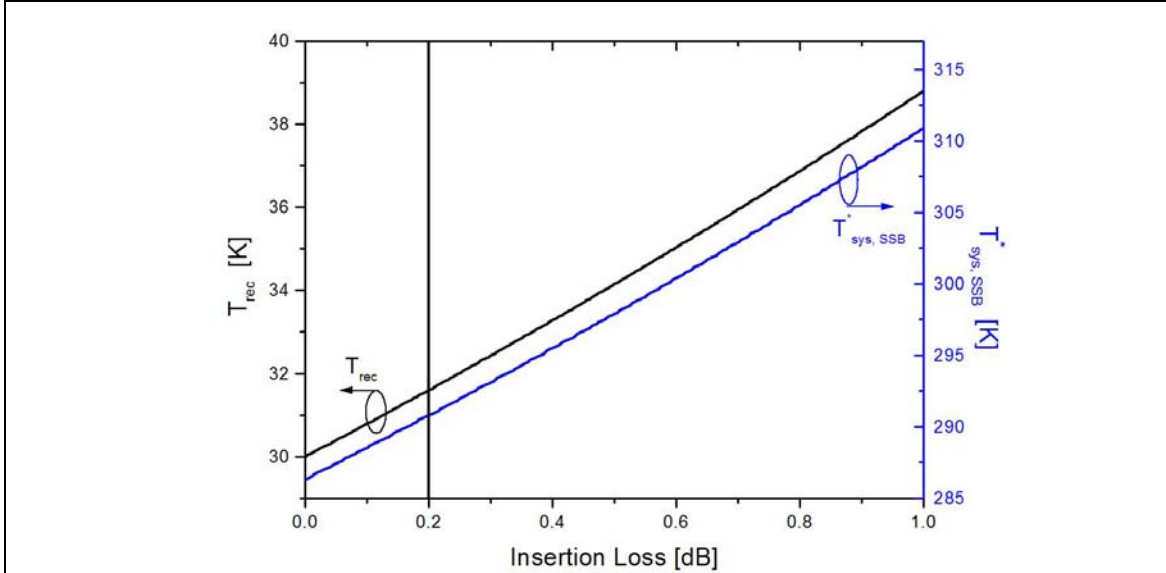


Fig. 21: Receiver (left scale) and system (right scale) noise temperature versus insertion loss of the OMT for typical operation at the CARMA site. The vertical line at 0.2 dB is the expected insertion loss of the OMT when operated at the physical temperature of 4 K.

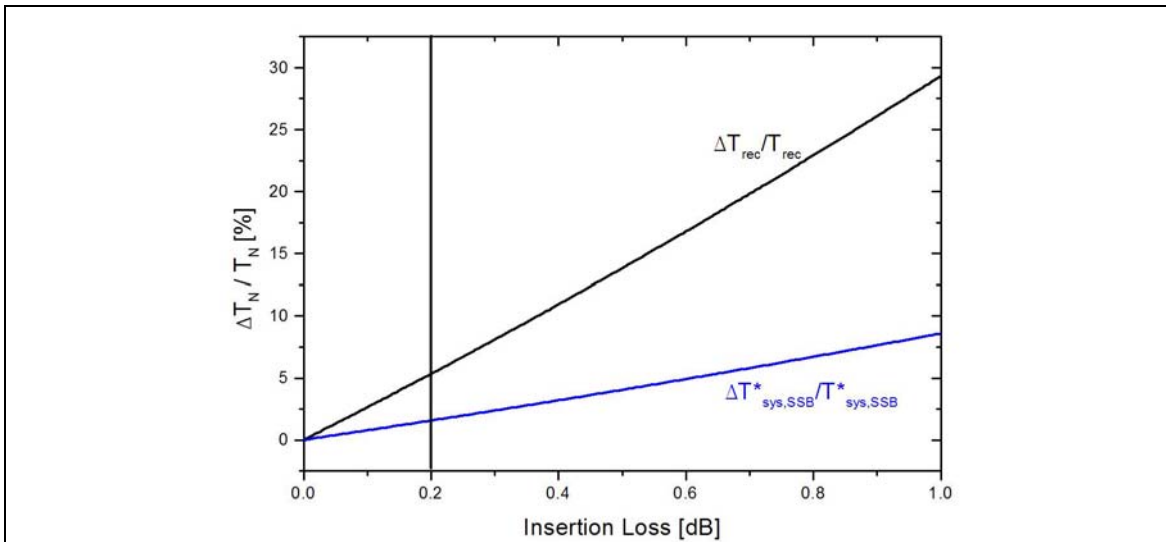


Fig. 22: Relative increase of receiver and system noise temperature versus insertion loss of the OMT.

insertion loss of the OMT (of about 0.6 dB) reduce to 0.2 dB after cooling at 4 K, we get:

$T_{\text{rec}}(\text{IL}=0.2 \text{ dB})=31.6 \text{ K}$ ,  $T_{\text{sys,SSB}}^*(\text{IL}=0.2 \text{ dB})= 290.8 \text{ K}$  that corresponds to relative variations  $\Delta T_{\text{rec}}/ T_{\text{rec}} =5.3 \%$  and  $\Delta T_{\text{sys,SSB}}^*/ T_{\text{sys,SSB}}^*=1.6 \%$ . Therefore, the increase of noise due to the OMT at 4 K degrades only slightly the sensitivity of a spectroscopic observation. If the two polarized signals were added together the net gain in sensitivity for spectral line and continuum observation would be about 40 %.

## 7 Conclusion

We tested five prototype turnstile junction waveguide orthomode transducers for the 1 mm band. Three of the OMTs have average room temperature insertion loss of ~1 dB or better, average input and output reflection of about -18 dB, and cross-polarization and isolation of order -30 dB over 210-270 GHz. The performance of the OMTs improved after filling small gaps between quadrants at the turnstile junction tuning stub with indium: the insertion loss decreased by several tenths of a dB across the band. The OMT that gave best performance has insertion loss better than 0.8 dB across 210-290 GHz. Two of the OMTs have deep resonances in the transmission. Electromagnetic simulations at 1 mm and experimentation with a scale model in K band of the OMT show that blocks misalignments due to fabrication errors or loose locating pins can cause these resonances. Use of dowel pins and holes with a tight fit in the inner part of the OMT may help solve this problem.

## 8 References

- [1] A. Navarrini, R.L. Plambeck, "A Turnstile Junction Waveguide Orthomode Transducer", IEEE Trans. Microw. Theory Tech., vol. 54, no. 1, pp. 272-277, Jan 2006.
- [2] A. Navarrini, R.L. Plambeck, and D. Chow, "A Turnstile Junction Waveguide Orthomode Transducer for the 1 mm Band", 16<sup>th</sup> International Symposium on Space Terahertz Technology, Gotenburg, Sweden, May 2-4, 2005.
- [3] A. R. Kerr, "Elements for E-plane split-blocks waveguide circuits," National Radio Astronomy Observatory, ALMA Memo n. 381, Jul. 2001. Available: <http://www.alma.nrao.edu/memos/html-memos/alma381/memo381.pdf>
- [4] CST Microwave Studio. Bűdinger Str. 2 a, D-64289 Darmstadt, Germany.
- [5] E. J. Wollack, W. Grammer, J. Kingsley, "The Bűifot Orthomode Junction", ALMA Memo n. 425, May 2002.